Biorefinery for heterogeneous organic waste using microbial electrochemical technology

Elie Desmond-Le Quéméner, Arnaud Bridier, Jiang-Hao Tian, Céline Madigou, Chrystelle Bureau, Yujiao Qi, Théodore Bouchez

Biorefinery for heterogeneous organic waste using microbial electrochemical technology

Elie Desmond-Le Quéméner[1,2], Arnaud Bridier[1], Jiang-Hao Tian[1], Céline Madigou[1], Chrystelle Bureau[1], Yujiao Qi[1], Théodore Bouchez[1]

[1]Irstea, UR HBAN, 1 rue Pierre-Gilles de Gennes, 92761 Antony cedex, France.
Corresponding author: theodore.bouchez@irstea.fr
[2]LBE, Univ Montpellier, INRA, Narbonne, France.

Keywords:

microbial electrolysis cell; microbial electrosynthesis; anaerobic digestion; environmental biorefinery

1 Abstract

Environmental biorefineries aim to produce biofuels and platform biomolecules from organic waste. To this end, microbial electrochemical technologies theoretically allow controlled microbial electrosynthesis (MES) of organic molecules to be coupled to oxidation of waste. Here, we provide a first proof of concept and a robust operation strategy for MES in a microbial electrolysis cell (MEC) fed with biowaste hydrolysates. This strategy allowed stable operation at 5 A/m^2 for more than three months in a labscale reactor. We report a two to four-fold reduction in power consumption compared to microbial electrosynthesis with water oxidation at the anode. The bioelectrochemical characterizations of the cells were used to compute energy and matter balances for biorefinery scenarios in which anaerobic digestion (AD) provides the electricity and CO_2 required for the MEC. Calculations shows that up to 22% of electrons (or COD) from waste may be converted to organic products in the AD-MEC process.

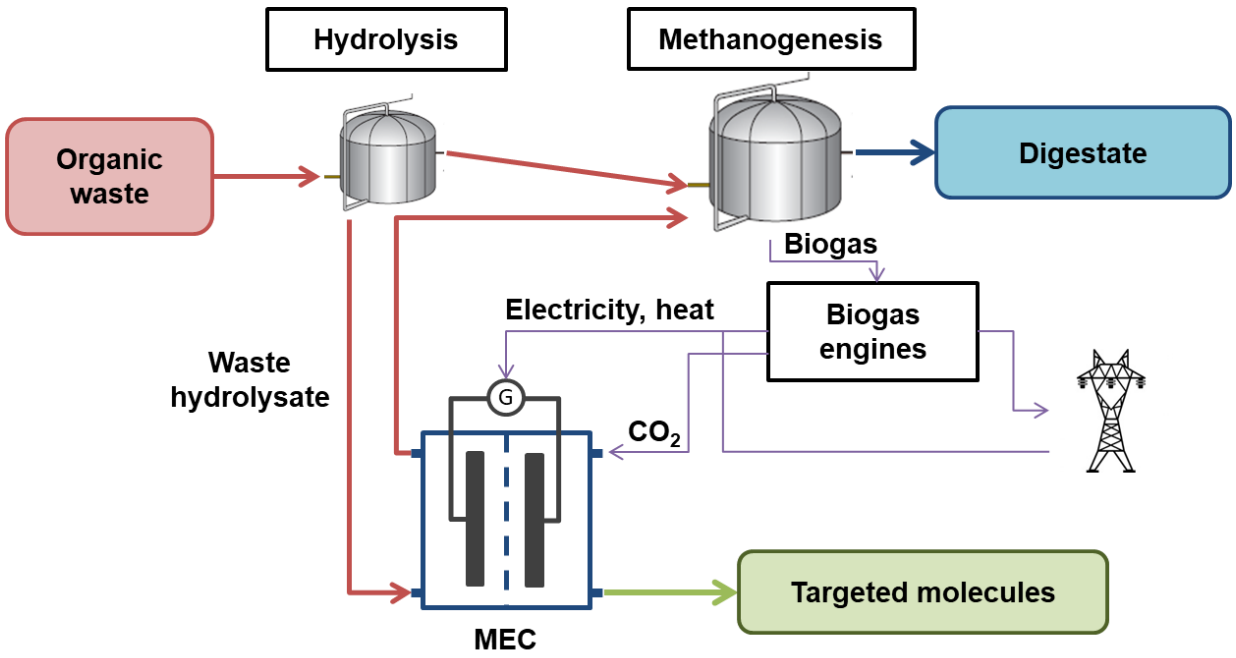

Figure 1: Schematic diagram of a waste biorefinery platform coupling a microbial electrolysis cell (MEC) with anaerobic digestion (AD) which is at the core of BIORARE (BIoelectrosynthesis for ORganic wAste bioREfinery) research project. The MEC selectively produces targeted molecules through microbial electrosynthesis (MES) in a cleaned controlled cathodic compartment using part of solubilized organic waste at the anode, while AD of the remaining waste produces biogas to be exploited as electrical power and heat to supply the MEC or for distribution to the utility grid.

1. Introduction

The increasing scarcity of resources and concerns about global warming are pushing our societies toward a circular economy in which wastes are recovered for reuse (Lieder and Rashid, 2016). In this context, biorefineries aimed at transforming biomass into fuels or chemicals could contribute to a sustainable supply of resources. Among biorefineries, environmental biorefinery technologies offer possibilities for sustainable waste remediation (Venkata Mohan et al., 2016). By combining treatment of wastes with production of added value molecules, these technologies represent a step toward the circular economy and more sustainable development. Currently, anaerobic digestion (AD) is a widely used technology for organic waste valorisation. However, the cost-effectiveness of this process is questionable because of the low value of its product, the biogas. An increasing number of researches are focused on new technologies able exploit the bio-resource in a more profitable way by producing high value chemicals such as multi-carbon organic molecules rather than methane.

The discovery of exoelectrogenic bacteria that are able to oxidize organic matter and use electrodes as electron acceptors led, in the past decades, to the development of microbial electrochemical technologies (METs). Diverse bacteria found in various habitats are indeed able to interact with anodes (Koch and Harnisch, 2016). Among them species such as *Shewanella oneidensis* and *Geobacter sulfurreducens* have been extensively studied, leading to the identification of pathways for extracellular electron transfer (Lovley, 2008). The developments in the field of METs led to the introduction of several applications that utilize waste oxidation by exoelectrogenic bacteria to fuel various technologies such as microbial fuel cells (MFCs), microbial electrolysis cells (MECs), microbial desalination cells (MDCs) etc…(Wang and Ren, 2013). With the discovery of microbial electrosynthesis (MES) in 2010 (Nevin et al., 2010), a paradigm shift has happened in the domain of METs with the possibility of producing soluble multi-carbons compounds from renewable electricity and CO_2 with high selectivity, high rate and with high energy efficiency. The process relies on the ability of microorganisms to reduce CO_2 to organic compounds with electrons derived from a cathode. The first report was by Nevin *et al*. on *Sporomusa ovata* (Nevin et al., 2010). Since then, other acetogenic bacteria with the same ability have been identified, e.g. *Sporomusa sphaeroides*, *Clostridium aceticum*, *Clostridium ljungdahlii*, and *Acetobacterium woodii* (Demler and Weuster-Botz, 2011; Nevin et al., 2011). Although the metabolic pathways of these electrotrophic bacteria remain largely unclear (Kracke and Kromer, 2014), microbial electrosynthesis offers a plethora of applications for green chemistry (Rabaey et al., 2011) with the possibility of producing different organic molecules such as fatty acids (acetate, butyrate or caproate) or alcohols (methanol, ethanol) from either defined co-cultures or environmental samples (Deutzmann and Spormann, 2017; Jourdin et al., 2018; Logan and Rabaey, 2012). With a suitable cathodic community, acetate could be produced at high rates (up to 0.69 kg m^{-2} day^{-1}) with 100% of e^- recovery (Jourdin et al., 2015). It could also be accumulated at high concentrations (up to 13.5 g L^{-1} until now) in a three-chamber reactor that advantageously uses the electric field and membranes to facilitate its extraction (Gildemyn et al., 2015).

The advantages of using waste oxidation at a bioanode to drive microbial electrosynthesis on a biocathode have been mentioned by several authors since 2010 (Hamelers et al., 2010; Rabaey and Rozendal, 2010; Sadhukhan et al., 2016). In particular, bioanode-biocathode coupling could provide an efficient way to reduce the energy demand of MES as demonstrated for the bioelectrochemical production of methane, hydrogen or caustic (Rabaey and Rozendal, 2010). Previous MES reports on studying the production of chemicals however focused on the cathode and all comprised an abiotic anode (Demler and Weuster-Botz, 2011; Deutzmann and Spormann, 2017; Gildemyn et al., 2015; Jourdin et al., 2018, 2015; Nevin et al., 2011,

2010), thus the experimental proof of concept of coupling microbial electrosynthesis to anodic waste oxidation is still lacking and the specific constraints that may arise from its implementation have never been evaluated. Indeed, in such a system, an appropriate balance should be struck between anodic and cathodic conditions for proper functioning. Importantly, anodic conditions should be kept in proper electrochemical potential range, namely between anodic potential superior to -0.4V (vs SHE) to allow the feasibility of the oxidation reaction, and inferior to +0.6V to prevent any risk of oxidative stress on the electroactive biofilm. Once these conditions are met, the conditions at the cathode are subjected to the influence of multiple factors among which the nature of catholyte, surface, material, geometry of electrode, biofilm activity and current intensity resulting from the anodic reaction. However, at the same time, optimal reduction rate at the cathode needs to be determined and maintained during the process to optimize MES as well as to avoid H_2 production which decreases the cathode's coulombic efficiency. This constraints explains probably why very little effort has been devoted to test the feasibility of performing MES in a MEC fed with waste streams as substrates, except for few theoretical studies (El Mekawy et al., 2016; Sadhukhan et al., 2016).

In this work, we report for the first time, the operation of a MEC oxidizing biowaste hydrolysate at the anode and synthesizing acetate and propionate at the cathode with a dedicated electrochemical control strategy to balance anodic and cathodic activities. Equilibrium between bioanode and biocathode activities was achieved through an automated regulation strategy able to deal with shocks caused by variation of biofilm activity or substrate deficiency. Experimental proof of concept was demonstrated at laboratory scale over several months of operation. Characterization of the yield and rates of the reactor were used for the development of a model that enables the simulation of performances achievable at larger scales and with various target molecules. This allowed us to evaluate an innovative environmental biorefinery scenario, in which a MEC is inserted as an additional block into an existing AD facility (Figure 1) and to compare its performances with other environmental biorefinery processes.

2. Materials and methods

2.1. Experimental set-up

The bioelectrochemical reactors consisted of custom H-cells with two 1.5 l glass chambers separated by a cation exchange membrane (CEM) (Fumasep® FKE, Germany) and sealed together with a clamping ring. Anodic compartments were inoculated with 1 cm × 1 cm pieces of anode from previous reactors fed with biowaste (Bridier et al., 2015). Cathodic compartments were inoculated with 100 ml of catholyte from reactors performing bioelectromethanogenesis in the lab. Anodic and cathodic compartments were then filled with biochemical methane potential (BMP) medium (NF EN ISO 11734) buffered with carbonates (8 g HCO_3^-/l) to reach a final working volume of 1 l. The anode was a 4 cm × 4 cm piece of carbon cloth (Paxitech®, France) connected to the external circuit by a platinum wire (Heraeus®, 0.5 mm). The cathode was a 4 cm × 4 cm stainless steel plate (Outokumpu®, 254 SMO, Germany) screwed onto a stainless steel shaft (DURAN® DU.1200386) bent into a J-shape. Both anodic platinum wire and cathodic stainless steel shaft were pushed through thick butyl rubber stoppers inserted in bottle caps.

The reactors were maintained at 35±2°C in a temperature regulated room and stirred with a magnetic stirrer. The anodic compartment was operated under N_2 atmosphere, and the cathodic compartment under a mixed 80/20 N_2/CO_2 atmosphere. The cathodic compartment was flushed with N_2/CO_2 gas mix at weekly intervals to ensure a supply of CO_2 to the cathodic microbes.

In the first series of experiments, two reactors were fed with 0.6 g acetic acid at the anode. In the second series of experiments, a third reactor was launched and regularly fed with 30 ml of reconstituted biowaste synthesized as described in a previous work (Bridier et al., 2015). Liquid samples (8 mL) were periodically removed through dedicated septa in the anodic and cathodic compartments and centrifuged at 10,000 g for 10 min. The resulting pellets and supernatant were stored separately at -20°C for analysis of biomass and chemical compounds, respectively.

Throughout the experiments, pH was manually maintained above 7.5 in the anodic compartment through manual addition of 1 ml of NaOH solution (0.5 mol/l) when it dropped below this threshold. Conversely, in the cathodic compartment, pH was manually maintained below 8.5 through manual addition of 1 ml of HCl solution (1 mol/l) when it rose above this threshold.

2.2. Electrochemical settings

Electrochemical experiments were performed using a multi-channel potentiostat (BioLogic®, France, VMP3, EC-Lab software) in a 3-electrode setup with anode as working electrode (Figure 2 top panel). Saturated calomel electrode (SCE, +0.24 V vs. Standard Hydrogen Electrode, SHE)(Radiometer Analytical) was used as reference electrode in the anodic compartment. Anodes were first polarized at +0.4 V vs. SHE at the beginning of the experiments. The method of control was switched from potentiostatic to galvanostatic when the current density reached 5 A/m^2 and this current density was maintained in the circuit. Finally, if an anode potential rose above +0.4 V vs. SHE, the control method was switched back to potentiostatic with anode polarization at +0.4 V vs. SHE (Figure 2 bottom panel) (Bouchez et al., 2016).

All potentials provided in this article refer to the standard hydrogen electrode (SHE) reference electrode.

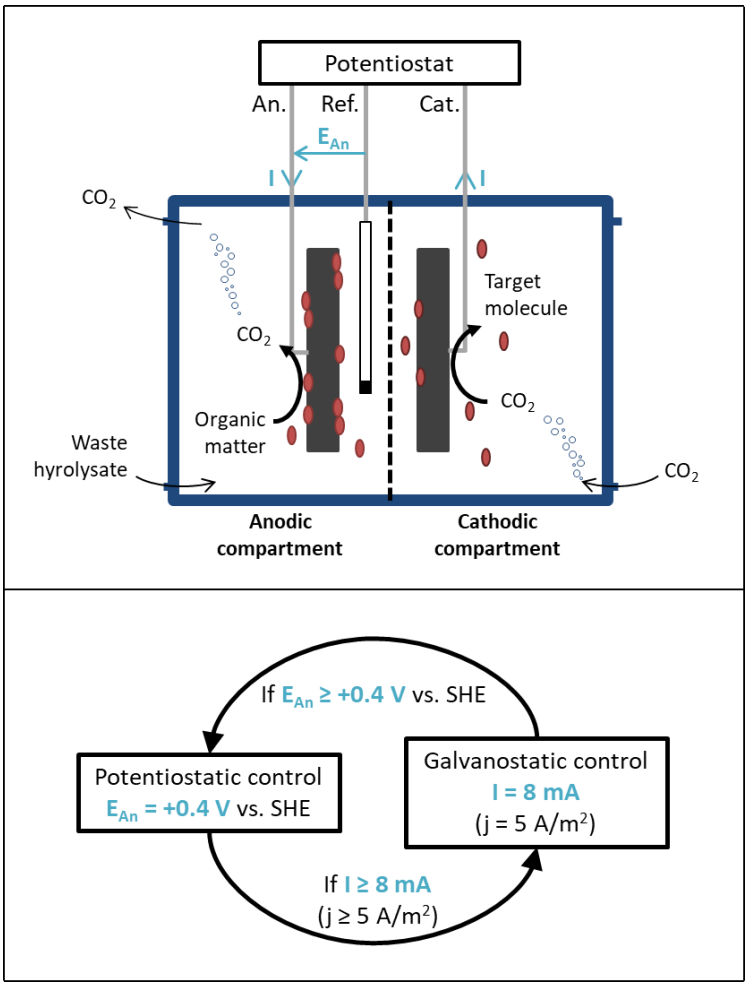

Figure 2: Experimental set-up (top panel) and control strategy (bottom panel) for microbial electrosynthesis (MES) in a microbial electrochemical cell (MEC). The cell (top panel) consisted in two chambers separated by a cation exchange membrane (CEM). Bacteria and archaea that catalyzed the reactions are illustrated in red. Electrochemical experiments were performed using a potentiostat and a 3-electrode setup with anode (An.) as working electrode, cathode (Cat.) as counter electrode and saturated calomel electrode as reference electrode (Ref.). E_{An} denote anode potential and I the current in the cell. The method of electrochemical control (bottom panel) alternated between potentiostatic control (E_{An} = +0.4 V vs. SHE) when anodic activity was low (I ≤ 8 mA i.e. current density below 5 A/m²) and galvanostatic control when the current density reached 5 A/m². During galvanostatic control if anodic potential reached +0.4 V vs. SHE, the control method was switched back to potentiostatic control.

2.3. Chemical analyses

The chemical oxygen demand (COD) of the anodic compartment fed with biowaste was measured using LCK514 kit (Hach Lange, range of measurement 100–2000 gO2/L). Acetate, propionate, butyrate, lactate, formate and valerate concentrations in the anodic and cathodic compartments were measured using ion chromatography (DIONEX DX 120, column IONPAC® ICE-AS1 (9x250 mm)). The mobile phases were heptafluorobutyric acid (0.4 mmol/L) and TBAOH (5 mmol/L). The apparatus was calibrated for measurement of concentrations ranging from 10 mg/L to 500 mg/L.

Biogas accumulation in the anodic and cathodic headspaces was measured using a differential manometer (Digitron 2082P). Gas compositions were determined using gas chromatography (Varian CP 4900). The three columns mounted on this device enabled the quantification of O_2, N_2, CH_4, CO_2, H_2, H_2S, and NO_2.

These data were used to calculate gas production and composition using the ideal gas law taking into account the extracted volume of gas and liquid samples.

2.4. Rates calculations

Through the manuscript two types of consumption and production rates are used. First, r_S are rates calculated relatively to electrodes projected surface. They are expressed in mol $e^-/m^2/d$, they allow checking electron balance and comparison with other METs. Second, r_V are rates calculated relatively to full reactor volume taking into account both anodic and cathodic compartments. They are expressed in $kg/m^3/d$ and allow comparison with other biorefinery technologies. Conversion between rates is calculated as follows:

$$r_V = r_S \cdot \frac{\frac{SV_{ratio} \cdot M}{2}}{\gamma \cdot 1000} \qquad (1)$$

where SV_{ratio} is the electrode surface to volume ratio (1.6 m^2 electrode per m^3 of anodic compartment for lab-scale reactors), M is the molecular mass of the considered compound, γ is its reduction degree in mol e^-/mol (calculated by writing the redox half reaction in which the compound is synthesized from CO_2), and 1000 is kg to g ratio.

2.5. Microbial analyses

Microbial analyses were performed on pellets recovered from the electrolyte samples and on biofilm samples from electrodes. Anodic biofilms were recovered by scratching and vortexing carbon cloth in a 150 mM NaCl sterile solution and then by centrifuging the resulting suspension. Cathodic biofilms were collected by scraping the electrode, rinsing with 1 mL of sterile water and centrifuging the resulting suspension.

Total DNA was extracted from the pellets using the Powersoil™ DNA isolation kit (MoBio laboratories) according to the manufacturer's instructions. DNA concentrations were quantified using a quantifying fluorescent dye assay (Qubit dsDNA BR assay kits) and Qubit 2.0 Fluorometer 180 (Invitrogen, Life Technologies. The V4 regions of 16S SSU rRNA gene were then amplified using the archaeal/bacterial primers 515F (5´-GTGCCAGCMGCCGCGGTAA-3´) and 928R (5´- CCCCGYCAATTCMTTTRAGT-3´) (Eurofins) and Platinium® Pfx DNA polymerase (Invitrogen, Life Technologies). Fusion primers were constructed according to the recommendations of the "Ion Amplicon Library Preparation (Fusion Method)." The sequences of barcodes were identical to those of "Ion Xpress ™ Barcode Adapters 1-96 Kit", which allows direct recognition of barcodes with a PGM sequencer. PCR reaction was performed using a Mastercycler Pro S thermocycler (Eppendorf) according to the following PCR conditions: 5 minutes at 94°C, followed by 30 cycles at 94°C for 15 seconds, 53°C for 30 seconds and 68°C for 1 minute, and a final elongation step at 68°C for 5 minutes. The PCR products were then checked by agarose gel electrophoresis and purified using Agencourt AMPure XP beads kit (Beckman-Coulter) according to the "Ion Amplicon Library Preparation (Fusion method)". The resulting libraries were then quantified using Agilent Bioanalyzer 2100 and the DNA 1000 kit (Agilent) according to manufacturer's instructions. The libraries were then diluted to 26 pM before being mixed in the same tube to be used for template preparation. Template was prepared with the Ion OneToucH_2 using the Ion PGM Template OT2 400 kit (Ion torrent) according to the manufacturer's instructions. Amplicons carried by the Ion sphere particles (ISP) prepared during the template preparation step were sequenced according to the "Ion PGM HI-Q Sequencing" protocol using a 316V2 chip and the Ion Torrent PGM™ platform (Ion Torrent, life technologies) at IRSTEA MIMOSE platform (Antony, France).

16S rRNA tag reads were analyzed with the UPARSE pipeline (Edgar, 2013) using USEARCH v8.0.1623 software. Short sequences with less than 300 bp were discarded, the remaining sequences were truncated to 300 bp and filtered for quality, keeping only those with expected errors < 1. Sequences were then dereplicated, and sorted by size to discard singletons. The high quality reads obtained were used for Operational Taxonomic Units (OTUs) clustering at 97% identity. Chimera were removed using UCHIME (Edgar et al., 2011) against the "gold" database (http://drive5.com/uchime/gold.fa) and a taxonomy was attributed for each OTU using the mothur method implemented in QIIME 1.8.0 (Caporaso et al., 2010; Schloss et al., 2009; Wang et al., 2007) against Silva database release 119 (Quast et al., 2013) with a minimum confidence of 0.8. OTU tables and taxonomy summary files were generated with QIIME. Additionally, BLAST searches (Boratyn et al., 2013) were performed against the refseq_rna database (Pruitt et al., 2007) to refine the taxonomic attribution of major OTUs analyzed in this paper.

2.6. Modelling

Models of MECs with either water oxidation or waste oxidation at the anode were developed to evaluate voltages for various MEC configurations (see calculations in supplementary material 1). Standard electrochemical equations were fitted on data measured with cyclic voltammetry on our experimental reactors (see supplementary material 2). Electrolyte conductivity and the distance between the electrodes were taken into account to calculate whole cell voltage *U* as a function of current density *j* as follows:

$$U(j) = E_{anode}(j) - E_{cathode}(j) + j\frac{d}{\sigma} \qquad (2)$$

where $E_{anode}(j)$ is the modeled anodic potential (using either a biotic anode model or an abiotic anode model), $E_{cathode}(j)$ is the modeled cathodic potential for the stainless steel electrode, d is the inter-electrode distance and σ is the electrical conductivity of the electrolyte.

These MECs models are used in part 3.4 for the evaluation of a waste biorefinery scenario where a MEC is integrated in an anaerobic digestion plant (see calculation in supplementary material 1).

3. Results and Discussion

3.1. Defining an electrochemical control strategy for coupled operation of bioanode and biocathode

The objective of this study was to conduct MES of soluble organic compounds from CO_2 in a MEC oxidizing waste. To achieve this, the electrical potentials and reactions rates at both anode and cathode need to be maintained within certain ranges. At the anode, the potential should not exceed +0,6V vs SHE to prevent oxidation of the anodic biofilm. At the cathode, the electron flux (current) in the system should be kept below the maximal electron processing rate for MES to prevent massive generation of H_2, which would decrease coulombic efficiency of the synthesis. To the best of our knowledge, this problematic has not been addressed yet, especially for long-term operation of MEC with MES at the cathode. In most bioelectrochemical studies at lab scale, potentiostatic control is used to have a precise control of working electrode potential versus a reference electrode. This strategy is obviously not adequate in our case. Indeed, if a potentiostatic control of the cathode is implemented, any variation of the anodic biofilm metabolic activity caused by lack of substrate or transient pH drop would be compensated by the potentiostat resulting in a sharp increase of the anode potential endangering the integrity of the anodic biofilm. Conversely, if an

anodic potentiostatic control strategy is implemented, the anodic activity may overflow the cathodic biofilm metabolic capacity resulting in electron loss through H_2 production. Here we report a strategy for preserving the anodic biofilm from oxidation risks while still achieving a galvanostatic control of the cell, i.e. maintaining a constant current in the cell. Galvanostatic control is indeed important as it enables controlling the electron flux at a rate compatible with MES. In addition, it is interesting for scale-up and industrialization since it allows maintaining a process with stable rates of waste oxidation and molecule production over time. The strategy developed is explained in materials and methods and in Figure 2 bottom panel. This strategy allowed low current densities when the anodic biofilm limited the flux of electrons, either due to its early stage of growth, or to substrate depletion or inadequate pH values (potentiostatic control phase); and allowed a limited maximum current density that matched the maximum electron processing rate of cathodic microbes (galvanostatic control phase).

3.1.1.First batch experiment: electromethanogenesis

Two MECs (cell 1 and cell 2) were conducted using the above strategy with 0.6 g/l acetate as anodic substrate. Results are shown in Figure 3. The current rose rapidly during the first period of potentiostatic control and reached 5 A/m^2 after 29 hours. The control method was then switched to galvanostatic and the anodic potential dropped to -0.2 V vs. SHE and remained stable for 7 to 9 days before an abrupt rise. The control method was then switched back to potentiostatic and the current decreased toward zero.

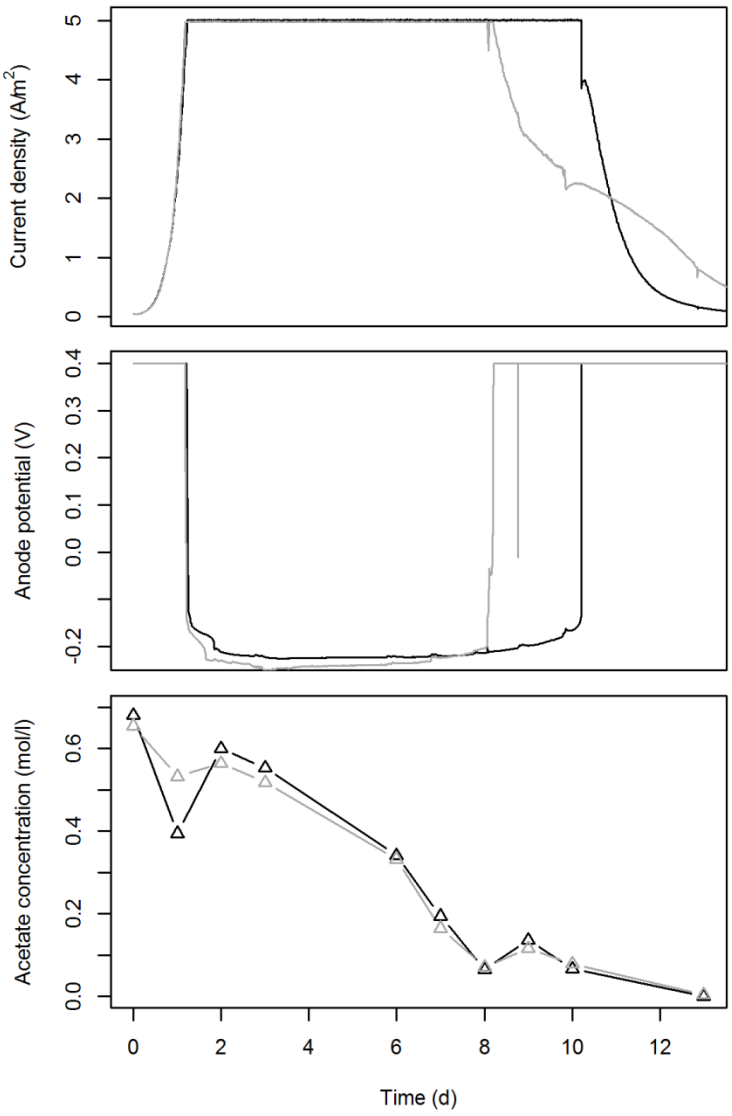

Figure 3: Current density (top panel), anode potential (middle panel) and acetate concentration in the anolyte (bottom panel) for two replicated MECs (cell 1 in black and cell 2 in gray) with a conduction strategy alternating potentiostatic control (potential fixed at 0.4 V vs. SHE at the beginning and at the end of the experiment) and galvanostatic control (fixed current density of 5 A/m^2) during the first batch experiment.

Acetate concentrations decreased concomitantly with current generation at the anodes (Figure 3 bottom panel). Overall coulombic efficiency (CE) for these bioanodes was 78.0±0.7%, with a mean rate of acetate consumption of 6.4 ± 0.5 mol e^-/m^2/d (0.038 ± 0.003 kg/m^3/d) between day 2 and day 8.

Gases and soluble compounds produced at the cathode during acetate oxidation are shown in Figure 4.

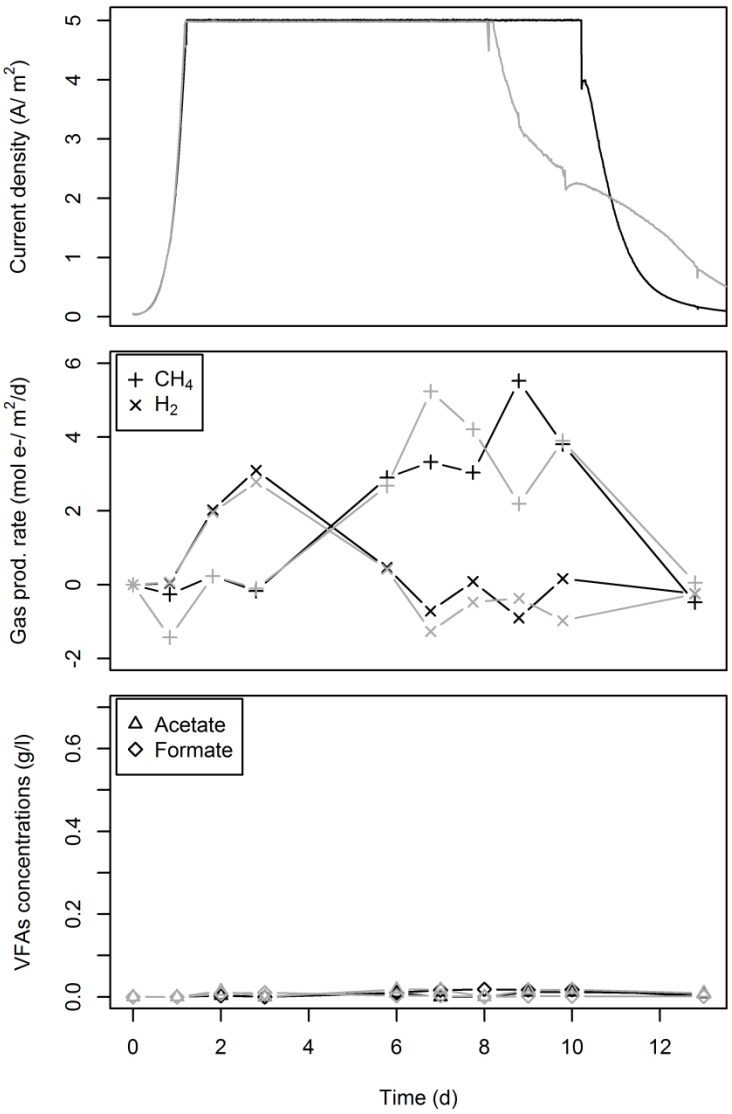

Figure 4: Current density (top panel), hydrogen and methane production rates (middle panel) and concentrations of major VFAs (acetate and formate) in the catholyte (bottom panel) for MECs 1 and 2 (black and grey curves respectively) during the first batch experiment.

Cathodic current resulted in hydrogen production at the cathodes during the first three days with a maximum rate of 2.9 ± 0.2 mol $e^-/m^2/d$ (0.002 $kg/m^3/d$). The cathodic potential was -0.75 V vs. SHE at that time compatible with abiotic water electrolysis to hydrogen on stainless steel. The hydrogen production rate then fell while methane production rate started to rise. It reached 5.4 ± 0.2 mol $e^-/m^2/d$ (0.009 $kg/m^3/d$) for both reactors between days 7 and 9, whereas, at the same time, hydrogen production rate was negative due to the consumption of hydrogen produced at the beginning of the experiment indicating a probable hydrogen route for methane synthesis in these reactors. The combined mean production rate of the two gases was 3.1 ± 0.8 mol $e^-/m^2/d$ for days 2 to 10 when the current density was 5 $A.m^2$ (4.5 mol $e^-/m^2/d$). The CE for gas production was then 74 ± 18%. No accumulation of volatile fatty acids was measured in the reactors (Figure 4 bottom panel) confirming that the majority of the electrons were used for methanogenesis.

3.1.2.Second batch experiment: inhibition of methanogenesis and production of VFAs

A second batch experiment was launched in cells 1 and 2 with a second injection of acetate in the anodic compartment to reach a final concentration of 0.6 g/l. The electrochemical conducting strategy was the same as the one described for the first experiment. A total of 10 mM 2-bromoethanesulfonate was added at the biocathode to inhibit methanogenesis (Marshall et al., 2012).

The current rose almost instantaneously after the addition of acetate (Figure 5 top panel) and the anodic CE reached 93.7±4.9% after 13 days, higher than measured in the first batch. This difference in CE between the first and second experiments was probably due to the difference in biofilm maturity. The anodic carbon cloth was clean at the beginning of the first batch experiment, whereas it was colonized by electroactive bacteria at the beginning of the second batch experiment.

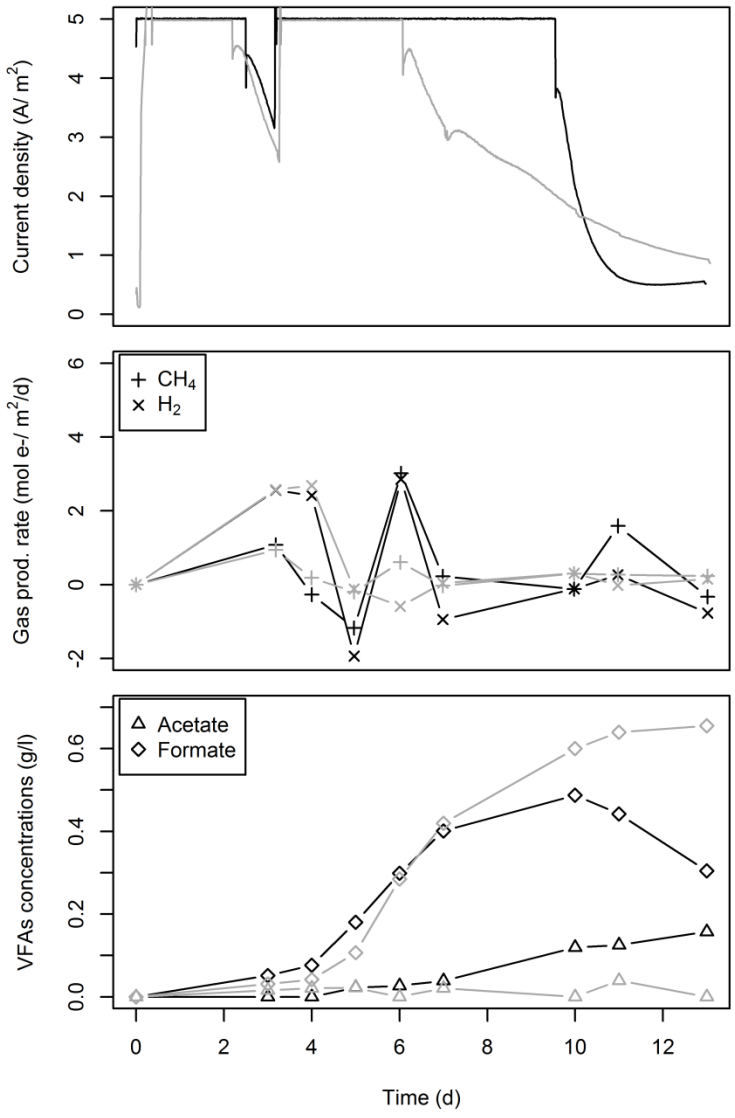

Figure 5: Current density (top panel), hydrogen and methane production rates (middle panel) and concentrations of major VFAs (acetate and formate) in the catholyte (bottom panel) for MECs 1 and 2 (black and gray curves respectively) during the second batch experiment.

The hydrogen production rate rose in the first 3-4 days and then fell to zero or to negative values (Figure 5 middle panel). The drop in the hydrogen production rate occurred at the same time as a rise in formate concentration in both reactors (Figure 5 bottom panel). Formate accumulated in cell 2 and reached a concentration of 0.66 g/l at the end of the experiment (day 13). In cell 1, it reached 0.49 g/l on day 10 and was then consumed. In this reactor, acetate was synthesized from day 6 on and reached 0.16 g/l at the end of the experiment. Between days 4 and 7, when current density was 5 A/m^2 in both reactors, the mean rate of formate synthesis was 3.3 ± 0.3 mol $e^-/m^2/d$ (0.059 ± 0.005 $kg/m^3/d$) corresponding to a CE of 74 ± 6%.

The strategy alternating potentiostatic and galvanostatic control thus enabled successful conduction of both biotic oxidation of acetate at the anode and electrosynthesis of organic molecules at the cathode of the MECs. The performances were much better than those previously documented for this type of reactor. For instance, Villano et al. and Xiang et al. reached 0.7 A/m^2 (calculated vs. projected surface area) and 0.4 A/m^2, respectively (Villano et al., 2011; Xiang et al., 2017), with comparable coulombic efficiencies, corresponding to a 10 times lower rate of synthesis.

3.2. Long term operation of a reactor fed with biowaste, and production of acetate and propionate

With this satisfactory conducting strategy and performance, a long term MEC was launched with biowaste fed at the bioanode. The whole experiment lasted three months. It was divided into five phases (I-V) with renewal of anode material and of 90 % of the catholyte at the end of each phase (days 8, 16, 25, 53 denoted t1-t4) and renewal of the anolyte on days 8, 16, 30, 42, 49 and 79. 30 ml of reconstituted biowaste was fed on days 0, 8, 16, 30, 42, 49, 67 and 79. Total chemical oxygen demand (COD) in the reactor as a function of time is shown in Figure 6 (top panel). Chemical analyses showed that 31-37% of the introduced COD was comprised of VFAs (3-4% acetate, 9-11% propionate and 17-21% butyrate; <1% formate) and 6-7% was comprised of lactate.

The first week was conducted without methanogenesis inhibition; 10 mM of 2-bromoethane sulfonate was then added in the catholyte at the beginning of every following phase (II-V) to inhibit methanogenesis.

3.2.1. Anode performances

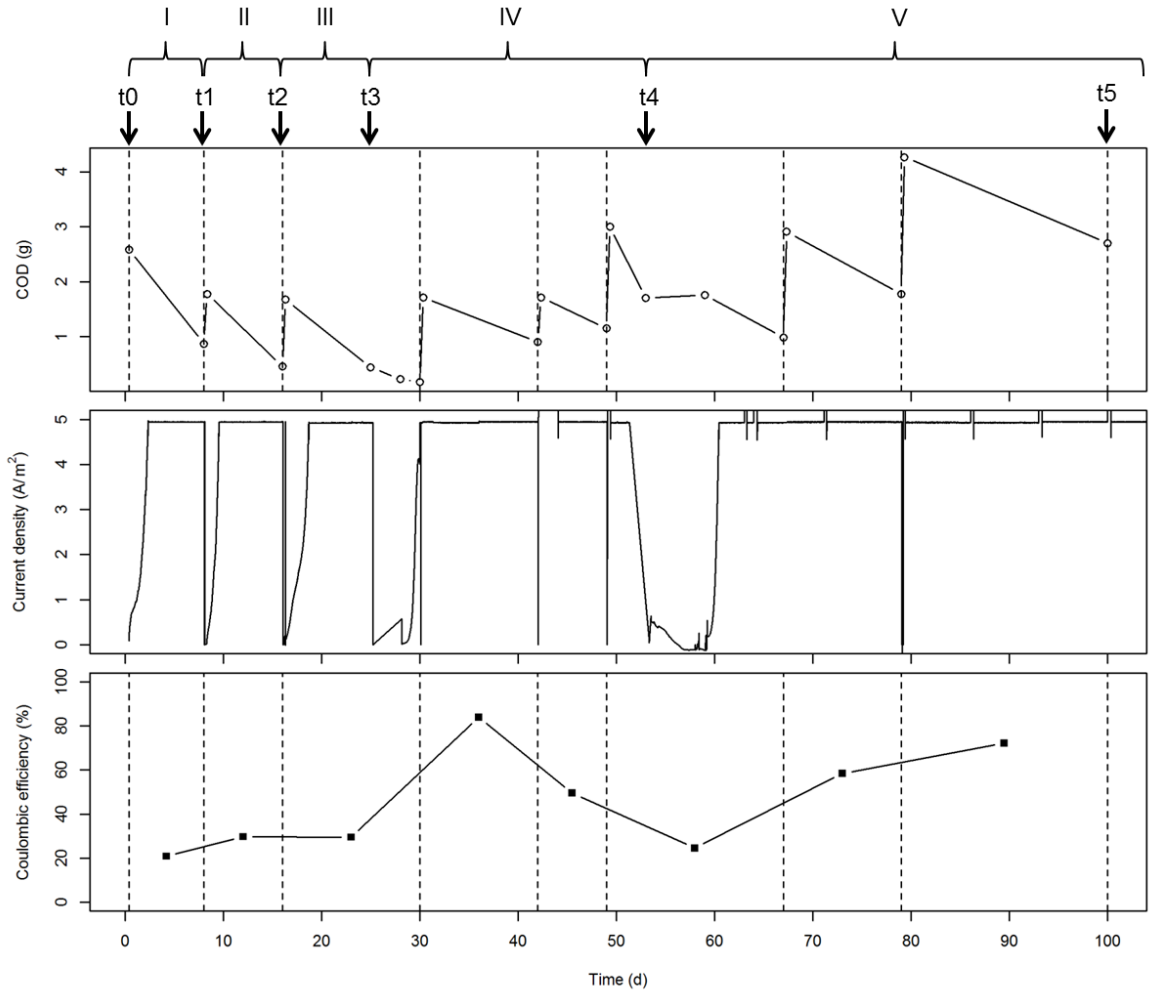

Figure 6: Total COD in the anodic compartment (top panel), current density (middle panel) and anodic coulombic efficiency (bottom panel) for the long term MEC. The 5 phases (I-V) correspond to phases with renewed anode material and catholyte (renewal at time t1-t4). Dashed lines show when 30 ml of reconstituted biowaste was added.

Coulombic efficiency (CE) was calculated for each feeding phase (delimited by dashed lines in Figure 6). CE was relatively low in the phases I-III (21 - 30%), it then reached 84% at the beginning of phase IV but decreased to 25% at the end of the phase. It finally recovered high stable values (58 - 72%) in the last phase.

These variations in CE can be linked to renewal procedures of anodic carbon cloth as discussed in a previous study (Bridier et al., 2015). The anodic biofilm probably reached maximum efficiency after three renewals of the carbon cloth and selection of efficient anodic microorganisms. The biofilm then lost some of its efficiency as it aged during phase IV but recovered its performance when the material was renewed at the beginning of phase V.

The maximum CE of biotic anodes observed in previous studies is provided in supplementary material 2. Current density and CE obtained here for the treatment of a complex biowaste appears interesting, however when taking into account the full volume of the reactor including both anodic and cathodic compartments, the bioelectrochemical treatment rate is low (0.029 kg COD/m^3/d). This is due to very low surface to volume

ratio for the anode in lab scale experiments (1.6 m^2/m^3). Possible scale-up and projected treatment rates are discussed below taking into account realistic surface to volume ratio (cf. part 3.4.3).

3.2.2. Cathode performances

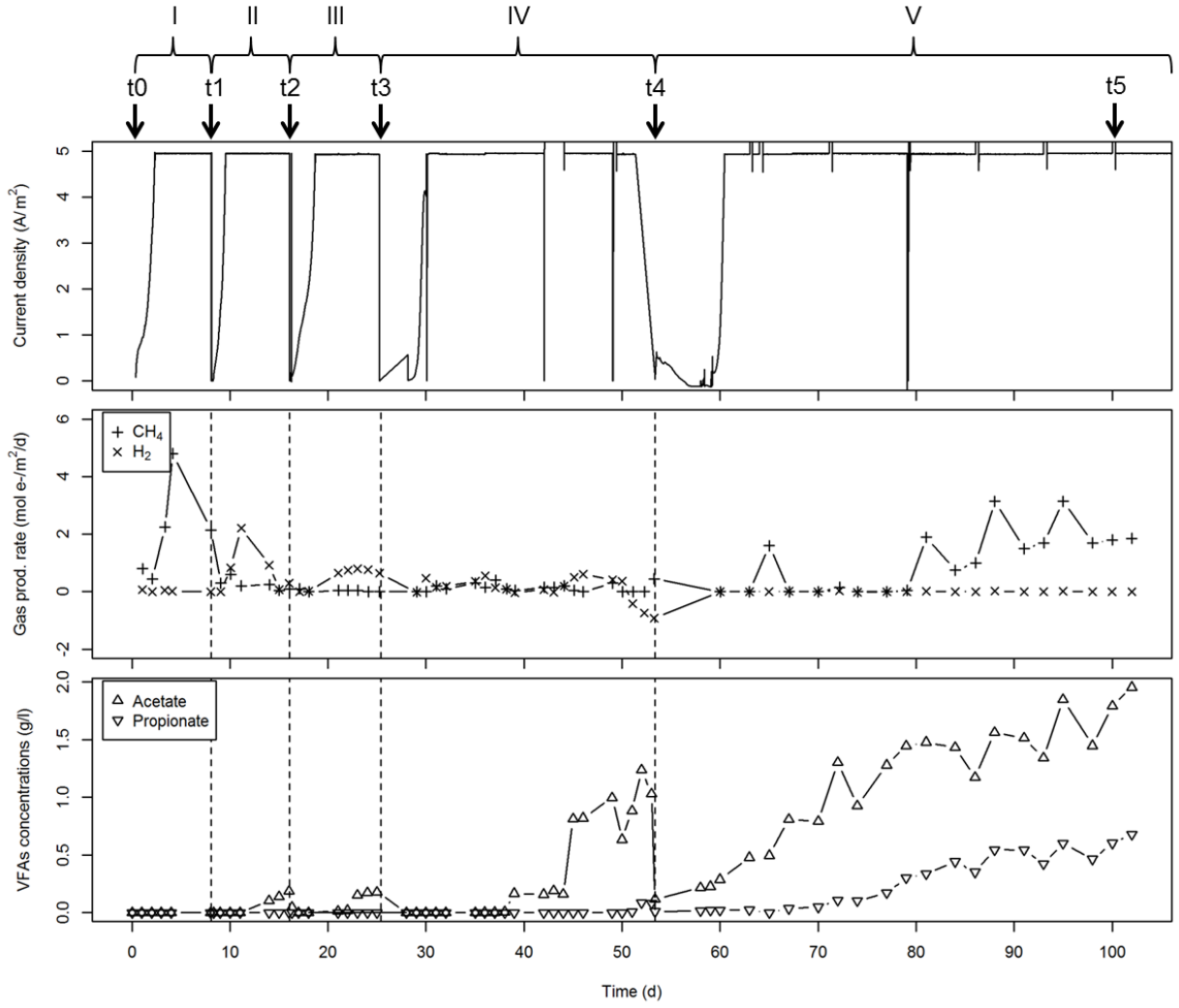

Figure 7: Current density (top panel), hydrogen and methane cathodic production rates (middle panel) and concentrations of major VFAs (acetate and propionate) in the catholyte (bottom panel) for the long term MEC. The 5 phases (I-V) correspond to phases with renewed anode material and catholyte (renewal times t1-t4 are indicated by the dashed lines).

Gas production rates and concentrations of acetate and propionate in the catholyte are shown Figure 7. In phase I, methane was the only product with a production rate of 3.1 ± 1.5 mol $e^-/m^2/d$ (0.005 ± 0.002 $kg/m^3/d$) for days 3 to 8 when the current density was 5 $A.m^2$ (4.5 mol $e^-/m^2/d$ or 0.029 kg $COD/m^3/d$). Coulombic efficiency (CE) for methane production was 68 ± 33%. During phase II, after addition of 10 mM BES to inhibit methanogenesis, hydrogen was first produced at a maximum rate of 2.2 mol $e^-/m^2/d$ (0.002 $kg/m^3/d$, 49 % CE) at day 11. Hydrogen production then decreased, and acetate was produced at a rate of 3.0 ± 0.1 mol $e^-/m^2/d$ from day 11 to day 16 (0.018 ± 0.001 $kg/m^3/d$, 68 ± 3 % CE). Hydrogen and acetate were again produced in phase III with respective production rates of 0.7 ± 0.1 and 4.0 ± 1.0 mol $e^-/m^2/d$ (0.001 $kg/m^3/d$, 16 ± 2 % CE and 0.024 ± 0.006 $kg/m^3/d$, 90 ± 22 % CE). During phase IV, after an initial lag time, acetate was the only product with a production rate of 4.5 ± 0.6 mol $e^-/m^2/d$ (0.027 ± 0.004 $kg/m^3/d$,

99 ± 13 % CE) from days 38 to 53 reaching a maximum concentration of 1.2 $g.l^{-1}$. Acetate production continued at a similar rate at the beginning of phase V until day 70. From day 79 to day 102, it slowed down to a lower rate of 1.6 ± 0.6 mol $e^-/m^2/d$ (0.009 ± 0.004 $kg/m^3/d$, 35 ± 14 % CE) and methane was again produced at a production rate of 1.8 ± 0.8 mol $e^-/m^2/d$ (0.003 ± 0.001 $kg/m^3/d$, 41 ± 17 % CE) despite the addition of BES, indicating probable adaptation of methanogenic populations to the inhibitor. Interestingly, methane production was accompanied by the production of propionate at a rate of 1.5 ± 0.4 mol $e^-/m^2/d$ (0.006 ± 0.002 $kg/m^3/d$, 24 ± 6 % CE). The final concentrations of acetate and propionate reached 1.9 and 0.7 g/l, respectively. Ethanol production was also detected (although below the quantification threshold) during phases IV and V, showing that the selected cathodic microbial community was also able to synthesize alcohols.

MES in a MEC fed with biowaste was thus successfully maintained on a long term, with stable operation at 5 A/m^2 (0.029 kg $COD/m^3/d$ with our lab-scale configuration) for long periods using the electrochemical control strategy explained above. MES production shifted first from hydrogen to acetate as reproducibly documented with short term and long term batch experiments. It then shifted to propionate over time with resurgence of methane production in the end of the experiment despite regular BES additions to inhibit methanogenesis. MES was very efficient with 99% CE during phase IV (0.027 $kg/m^3/d$ acetate production rate). Analyses of the microbial communities at different time points were then performed to more thoroughly understand anodic performances and metabolisms observed at the cathode.

3.3. Microbial community

3.3.1. Anodic biofilm

Microbial communities from the anodic biofilm and from suspended biomass sampled at time t1 (day 8) were investigated using 16S rRNA amplicon sequencing. The relative abundance of the main genera are shown in Figure 8.

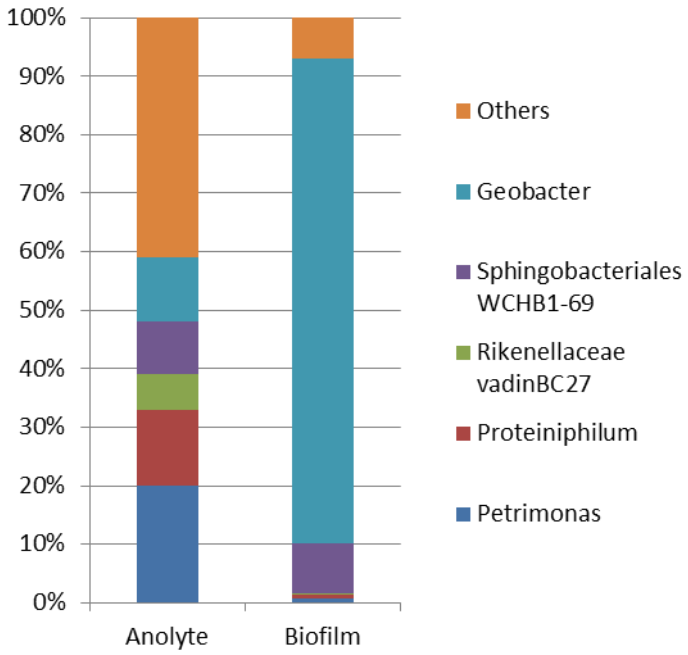

Figure 8: Compositin of the microbial community of the anolyte and of the anodic biofilm identified from 16S sequences. Only genera with relative abundances above 5% in at least one sample are shown.

Genus *Geobacter* (phylum Proteobacteria, order Desulfuromonadales) was highly dominant in the biofilm with a relative abundance of 83% at the electrode. Blast results showed that the corresponding sequences shared 99% identity with *G. anodireducens* and *sulfurreducens*, both of which are prominent electroactive species. The only other major phylum identified in the biofilm was WCHB1-69 (phylum Bacteroidetes, order Sphingobacteriales) with a relative abundance of 8%. These results are very similar to those obtained from biowaste oxidizing bioanodes developed from the same inoculum and published in a previous study (Bridier et al., 2015). The phylum that was identified here as WCHB1-69 was previously identified as Vc2.1 bac22. The differences in the assignments are probably due to the differences in the databases used. The high dominance of *Geobacter sulfurreducens* here is not surprising at it has often been found to be dominant in mixed anodic biofilms oxidizing organic matter and is known to form thick biofilms on anodes fed with acetate (Torres et al., 2009). Acetate was one of the major metabolite found in the biowaste hydrolysate used in the experiments and was also probably produced by the suspended microbial community through fermentation.

The suspended microbial community was more diverse than the biofilm with five major phyla identified: *Petrimonas* (phylum Bacteroidetes, order Bacteroidales), *Proteiniphilum* (phylum Bacteroidetes, order Bacteroidales), *Geobacter* (phylum Proteobacteria, order Desulfuromonadales), WCHB1-69 (phylum Bacteroidetes, order Sphingobacteriales), vadinBC27 wastewater-sludge group (phylum Bacteroidetes, order Bacteroidales). Again, these results are very similar to those obtained from biowaste oxidizing bioanodes developed from the same inoculum and published in a previous study (Bridier et al., 2015). The good anodic performances reported above probably resulted from a commensal interaction between the abundant Bacteroidetes in the anolyte able to consume complex substrates and to produce easily degradable substrates such as acetate or hydrogen, which are highly favorable substrates for the *Geobacter* species dominating the biofilm.

3.3.2. Cathodic microbial community

DNA was recovered from liquid samples at the end of phases I to V (days 8, 16, 25, 53 and 100 denoted t1-t5). DNA was only recovered from the biofilm at days t1, t3 and t5 in order to avoid disturbing the attached microbial ecosystem too frequently. Microbial communities where then assessed from 16S rRNA amplicon sequencing. Results are shown in Figure 9.

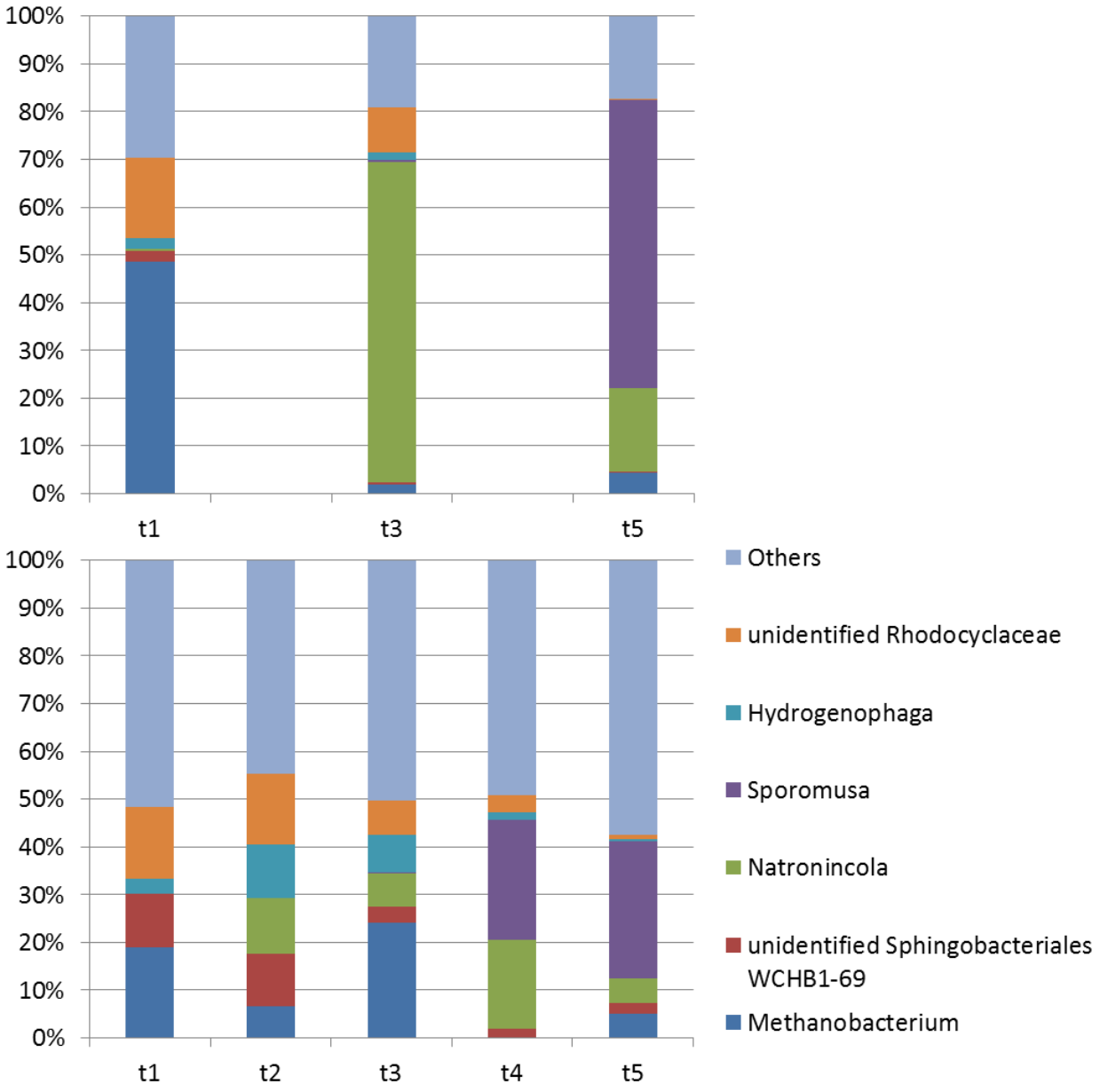

Figure 9: Composition of the microbial community in the cathodic biofilm (top panel) and catholyte (bottom panel) identified from 16S sequences at days t1-t5. Only major genera with relative abundances above 10% in at least one sample are shown.

There was a clear switch between three major genera dominating biofilm populations at time t1, t3 and t5 (Figure 9 top panel). *Methanobacterium* dominated the community at t1 with a relative abundance of 49%, then *Natronincola* dominated at time t3 with a relative abundance of 67% and finally *Sporomusa* dominated

at time t5 with a relative abundance of 60%. Community composition of the catholyte confirmed these population dynamics with the dominance of *Methanobacterium* at t1 followed by the appearance of *Natronincola* (t2-t5) and *Sporomusa* (t4-t5) (Figure 9 bottom panel).

These ecological successions were correlated with the shifts in metabolic products reported above. The dominance of *Methanobacterium* at the beginning of the experiment was associated with a phase of electromethanogenesis. This is congruent with other studies reporting the presence of *Methanobacterium* on biocathodes reducing carbon dioxide to methane (Koch and Harnisch, 2016). After the addition of BES, the methanogenic population in the biofilm shrank to only 2% and 4% of the community at t3 and t5, respectively, in accordance with gas measurements indicating null or low methane production for the rest of the experiment. Interestingly, the low resurgence of methane production in the end of the experiment may be linked to a shift in *Methanobacterium* OTUs dominating the archaeal population (see supplementary material 2). After BES addition, the microbial population was dominated either by *Natronincola* or *Sporomusa* during a phase of VFA (acetate, propionate) production. *Sporomusa* has been repeatedly identified in acetogenic biocathodes and is a known electroactive bacterium (Koch and Harnisch, 2016; Nevin et al., 2010), but, to our knowledge, the genus *Natronincola* has never been reported in acetogenic biocathodes. This particular genus was also dominant in the catholyte in the short term experiments after BES inhibition (data not shown). The best BLAST hit of its representative sequence against refseq_rna database was *Natronincola peptidivorans* strain Z-7031 (99% identity), an anaerobic alkaliphilic peptolytic iron-reducing acetate producing *Clostridia* isolated from soda lakes (Zhilina et al., 2009). Interestingly, the optimum pH reported for it is close to the pH of 8.5 maintained in our catholytes. However *Natronincola* has never been reported to be able to fix CO_2, to utilize H_2 or for direct electron transfer. Its alkaliphily and halotolerance are attractive characteristics for an electro-synthesizing microbe, as microbial electrosynthesis consumes protons, and as electrochemical efficiency is favored in high salinity media due to low ohmic losses. It is thus an interesting new potential electro-synthesizing bacterium in the family *Clostridiaceae*.

3.4. Modelling new environmental biorefinery scenarios including MEC

3.4.1. Power consumption

Using waste oxidation at the anode rather than water oxidation to fuel MES at the cathode allows reducing electrical power consumption for the synthesis. To evaluate this power gain, power inputs for reactors oxidizing either waste on a bioanode or water on a platinum abiotic anode were measured for current densities up to 25 A/m^2 (Figure 10).

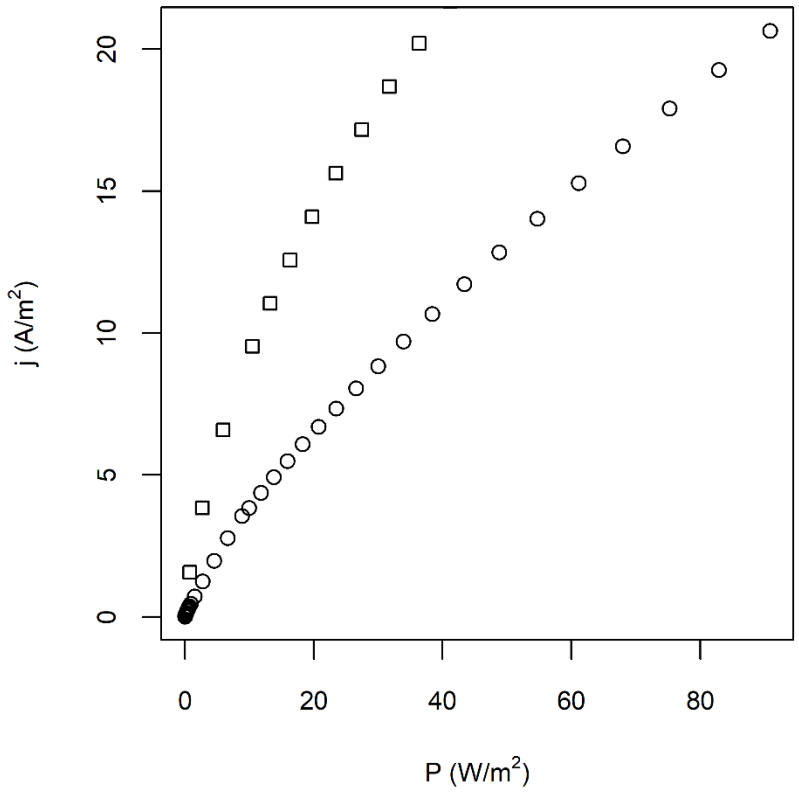

Figure 10: Evolution of current density as a function of electric power input for two H-type MEC comprising a microbial electrosynthesis biocathode. Square symbols corresponds to a MEC comprising a mature electroactive biofilm oxidizing waste at the anode, circles correspond to a MEC comprising an abiotic platinum anode oxidizing water.

As expected, the power density required to sustain a given current density was higher with a cell comprising an abiotic platinum anode than with a MEC oxidizing waste, indeed the potential for water oxidation is around 1.5 V above the potential of organic acid oxidation (Rabaey and Rozendal, 2010). The power required decreased by a factor ranging from 3.3 to 2.4 for current densities between 5 A/m^2 and 20 A/m^2. Performing MES in a MEC fed with waste thus allows notable savings in electricity in comparison with performing MES with water oxidation at the anode. This is a major advantage of this technology as electricity costs are the main cost of current systems for MES (Conrado et al., 2013).

To more thoroughly study the potential gain provided by a MES in a MEC vs. MES with water oxidation at the anode and the influence of various design and operating parameters on performance, a model was developed using standard electrochemical equations fitted on data measured with cyclic voltammetry on our experimental reactors (see supplementary material 2). The overall model was validated using the power measurements shown in Figure 10. This model makes it possible to extrapolate power gains for various cell configurations. Results are shown in Table 1 for a given electrolyte conductivity and for various inter-electrode distances and current densities.

Table 1: Power gain for MES in a MEC vs. MES with water oxidation at the anode for different anode-cathode distances and current densities with given electrolyte conductivity. For example, at 1 A/m^2 and with an inter-electrode distance of 0.01 m

one needs to invest 4.2 times less power to fuel MES in a MEC than MES with water oxidation at the anode. The dark red to white colors correspond to high to low power gain.

		j (A/m²)					
		1	5	10	15	20	25
d (m)	0.01	4.2	3.6	3.2	2.9	2.6	2.4
	0.05	4.1	3.4	2.9	2.6	2.3	2.1
	0.1	4.0	3.1	2.6	2.3	2.1	1.9
	0.15	3.9	2.9	2.4	2.1	1.9	1.7
	0.2	3.8	2.8	2.2	1.9	1.8	1.6
	0.25	3.7	2.6	2.1	1.8	1.7	1.5
	0.3	3.7	2.5	2.0	1.7	1.6	1.5

It shows that the power gained using a bioanode vs. Pt anode is maximum with a low current and short interelectrode distance and decreases with increasing current density or distance between electrodes. With low interelectrode distances (1 to 5 cm) the gains are interesting with a minimum gain of 2.1 (i.e. at 25 A/m^2 and a maximum gain of 4.2 for 1 A/m^2. For reactors with a less optimal configuration (longer distance between the electrodes) the advantage of using a bioanode is less with a power gain as low as 1.5 for 25 A/m^2 due to the prevalence of ohmic losses.

3.4.2. Target molecules and rates

In terms of production rate and carbon fixation rate of the MEC, performances depend only on current density, coulombic efficiency and on the chemical properties of the target molecule. The rates are, indeed, directly proportional to the ratio of mass to the degree of reduction (M/γ) and of the carbon mass to the degree of reduction (C-M/γ), respectively, where the reduction degree γ represents the amount of electron available in a compound. Its value is easily calculated by writing the redox half reaction in which the compound is synthesized from CO_2. Ratios and rates are shown in Table 2 for an current density of 10 A/m^2 and a cathodic coulombic efficiency of 90% for a wide diversity of molecules ranging from gases (methane and hydrogen) to medium-chain fatty acids (caproic acid). Detailed calculations are provided in supplementary material 1.

Table 2: Predicted synthesis rate of different molecules at a given current density (10 A/m²) and cathodic coulombic efficiency (90%). Rates are calculated respectively to the projected surface of electrodes.

Target molecule	M/γ (g/mol e-)	Synthesis rate (kg/y/m²)	C-M/γ (g C/mol e-)	Carbon fixation rate (kg C/y/m²)
Hydrogen	1.00	2.94	0.00	0.00
Methane	2.00	5.88	1.50	4.41
Ethanol	3.83	11.28	2.00	5.88
Butanol	3.08	9.07	2.00	5.88
1,3-propanediol	4.75	13.97	2.25	6.62
Formic acid	23.00	67.66	6.00	17.65
Acetic acid	7.50	22.06	3.00	8.82

Propionic acid	5.29	15.55	2.57	7.56
Butyric acid	4.40	12.94	2.40	7.06
Caproic acid	3.63	10.66	2.25	6.62
Lactic acid	7.50	22.06	3.00	8.82
Succinic acid	8.43	24.79	3.43	10.09
Citric acid	10.67	31.38	4.00	11.77

Table 2 shows that the best molecules to obtain high synthesis rates are molecules with a high M/γ ratio, i.e. oxidized molecules such as formic acid, citric acid or succinic acid. In a MEC, the total mass of product synthesized per year will then only depend on the amount of organic waste available as a feedstock.

3.4.3. Waste biorefinery with a MEC integrated in an anaerobic digestion (AD) plant

The size and productivity of a MEC can be evaluated for a defined amount of waste. For example, for the treatment of 100,000 t of waste per year with a BMP of 100 m^3/t of which 40% is used by the bioanode at 10 A/m^2 and 60% coulombic efficiency, the anodic surface is evaluated to 230,000 m^2. Thus for a surface to volume ratio of 40 m^2/m^3, as documented for carbon cloth (Janicek and Fan, 2014), the volume of the anodic compartment would be 5,700 m^3, which corresponds to a big anaerobic digestion unit. In terms of waste treatment rate this corresponds to 1.4 kg COD/m^3/d when reported to total reactor volume in line with rates estimated in a previous study (Bridier et al., 2015). This corresponds to standard treatment rates documented for the anaerobic digestion or for the dark fermentation of food waste (Capson-Tojo et al., 2016). This rate could be optimized using different type of electrodes such as carbon brush which allows higher surface to volume ratio up to 120 m^2/m^3 (Janicek and Fan, 2014) thus potentially reaching higher treatment rates up to 4.3 kg COD/m^3/d. These projected treatment rates appear encouraging with performances comparable with known technologies for food waste treatment, however MEC technology is still very young and performances at large scale remains to be evaluated and optimized. In terms of synthesis rate, with a cathodic coulombic efficiency of 90%, the rate would then be 1.3 to 3.9 kg COD/m^3/d when reported to total volume. Production rates calculated for various compounds with the above mentioned parameters are shown in Table 3. However, independently of this cathodic synthesis rate, the amount of molecule ultimately produced would only depend on the amount of waste available. Estimations of annual amounts of products and of carbon emitted are listed in Table 3.

Table 3: Estimations of annual amounts of products, of CO_2 emitted and of savings in CO_2 emissions as a function of the target molecules

Target molecule	Production rate (kg/m^3/d)	Annual production (kt/y)	Emitted CO_2 (kt C/y)	Savings in CO_2 emissions compared to anaerobic digestion (kt C/y)
Hydrogen	0.08	0.7	7.0	0.0
Ethanol	0.31	2.6	5.7	1.3
Butanol	0.25	2.1	5.7	1.3
1-3,propanediol	0.38	3.2	5.5	1.5
Formic acid	1.90	15.5	3.0	4.0
Acetic acid	0.60	5.1	5.0	2.0

Propionic acid	0.43	3.6	5.3	1.7
Butyric acid	0.35	3.0	5.4	1.6
Caproic acid	0.29	2.4	5.5	1.5
Lactic acid	0.60	5.1	5.0	2.0
Succinic acid	0.68	5.7	4.7	2.3
Citric acid	0.86	7.2	4.3	2.7

The MEC requires electricity and heating, so, given that only a fraction of waste is used at the anode (40% of the BMP, see above) an interesting scenario would be to couple this bioelectrochemical system to anaerobic digestion (AD), which would send electricity, heat and CO_2 produced from biogas to the MEC (denoted AD-MEC process, see Figure 1, calculations are included in supplementary material 1). Such a scenario indeed holds a great potential from an environmental point of view as revealed by life cycle analysis (Foulet et al., 2018). With this scenario, the fraction of COD (or electrons) from waste converted to products is maximized as the electricity produced from biogas would be almost entirely (96%) consumed for the production of molecules. This shows that, considering the parameters mentioned above, up to 22% of the COD may be converted to organic molecules produced in the MEC powered by AD. In that case, the power consumed by the MEC is 19 GWh/y. In comparison, MES with water oxidation at the anode would consume 2.9 times more power for the same amount of products (cf. Table 1) *i.e.* 56 GWh/y, and electricity produced from AD of 100% of the waste as a separate process would produce only 34 GWh/y (cf. calculations in supplementary material 1). Thus, the production of molecules using AD and MES separately instead of the integrated AD-MEC process would require either 1.6 times more waste or an additional electrical input of 22 GWh/y. Since electric power consumption represents about two thirds of the cost of the molecules produced by MES systems (Conrado et al., 2013; El Mekawy et al., 2016), this is a decisive breakthrough for microbial electrochemical technologies in terms of potential economic profitability. On the basis of the estimates made by El Mekawy *et al.*, the operational expenditures of such a low energy consuming MES in a MEC process could be as low as 0.14-0.33 €/kg (depending on the type of molecule produced), which could render the production of simple commodity molecules such as formate or acetate profitable (El Mekawy et al., 2016).

Balances also show that CO_2 is not limiting in the AD-MEC process (cf. Table 3). AD, biogas burning and anodic oxidation of waste advantageously provide plenty of CO_2 that may be fed to the cathodic compartment of the MEC. This, in turn, means that the AD-MEC process doesn't allow net fixation of CO_2 due to this excess of CO_2. Emissions will however still be reduced by up to 57% when compared to AD alone as shown in Table 3. Indeed, part of the carbon originally found in the waste is captured in the organic products of the AD-MEC process. Complete capture of emitted carbon might be obtained with the additional use of MES with water oxidation at the anode. This will however be only possible at the expense of additional electrical input.

The AD-MEC process can also be compared to more conventional waste biorefinery processes in which organic acids and biogas are directly produced by fermentation. For example Kim *et al*. proposed a bioprocess for the production of both lactic acid and biogas from food waste with increased economic benefit in comparison with exploitation of biogas only (Kim et al., 2016). Using food waste with a BMP of 112 m^3/t these authors reported production of 47 kg of lactic acid per ton of food waste and 54 m^3 of biogas. In comparison, the model of an AD-MEC process predicts production of 51 kg of lactic acid per ton of

biowaste with a BMP of 100 m^3/t but no production of biogas which is almost completely consumed for power generation MEC. In this case the AD-MEC process appears to be less advantageous than the fermentation process, as the slightly higher production of lactic acid would not compensate for the lack of biogas (4 USD for 4 kg lactic acid vs. 13 USD for 54 m3 of biogas (Kim et al., 2016)). This result is expected, since simple fermentation of biowaste involves fewer transformation steps, and hence less energy dissipation, than MES in a MEC in which target molecules are synthesized from CO_2. Despite this disadvantage, MES in a MEC present several appealing advantages. First, the process might benefit from in situ extraction of products thanks to a dedicated design of the electrochemical system. For example, Gildemyn *et al*. used a reactor with three chambers: an anode chamber, a cathode chamber and a central chamber for extraction (Gildemyn et al., 2015). The membrane separating the anode chamber from the central chamber was a cation exchange membrane (CEM), while the membrane separating the central chamber from the cathode chamber was an anion exchange membrane (AEM). Thus, when water was oxidized at the anode and protons were released into the solution, the negatively charged species, such as acetate produced at the biocathode, moved from the cathode chamber to central chamber. This allowed recovering acetate in the central chamber as an acidified stream containing up to 13.5 g/l. Second, the most appealing advantage of the process resides in the physical separation between anodic compartment receiving waste and cathodic compartment where target molecules are synthesized. This physical separation prevents potential contamination of products with any pollutants that might be present in wastes, and most importantly it introduces the possible usage of pure cultures (Nevin et al., 2011), of genetically engineered microorganisms (Straub et al., 2014), or of selected ecosystems (Jourdin et al., 2018) for the biorefinery of waste. This might be a decisive advantage when compared to current mixed culture processes that are driven by the endogenous microbial communities found in waste. This could thus be a technological breakthrough and open the door to the biorefinery of biowaste with selective synthesis of molecules such as succinic acid of higher economic value (Table 2Table 2 and Table 3).

4. Conclusions

Here we present the first proof for a microbial electrolysis cell (MEC) in which the biological oxidation of biowaste at the anode is coupled to the production of organic molecules by microbial electrosynthesis (MES) at the cathode. Compared to MES with water oxidation at the anode, this implementation enables an up to four-fold reduction in electric power consumption which is a decisive breakthrough in terms of potential economic profitability. Furthermore, we studied scenarios in which MES in a MEC is coupled to an anaerobic digestion facility. The results confirm the potential of MEC to become a cornerstone of environmental biorefineries.

E-supplementary data for this work can be found in e-version of this paper online

2 Acknowledgments

The authors would like to thank the anonymous reviewers who worked on this manuscript for their critical reading. Many useful suggestions were made and helped improve the text. The authors would also like to thank French National Research Agency for supporting the BIORARE project (ANR-10-BTBR-02).

3 References

Boratyn, G.M., Camacho, C., Cooper, P.S., Coulouris, G., Fong, A., Ma, N., Madden, T.L., Matten, W.T., McGinnis, S.D., Merezhuk, Y., Raytselis, Y., Sayers, E.W., Tao, T., Ye, J., Zaretskaya, I., 2013. BLAST: a more efficient report with usability improvements. Nucleic Acids Res. 41, W29–W33. https://doi.org/10.1093/nar/gkt282

Bouchez, T., Bridier, A., Le Quéméner, E., 2016. Method and device for controlling the activity of a bioelectrochemical system comprising both a bioanode and a biocathode. WO/2016/051064.

Bridier, A., Desmond-Le Quemener, E., Bureau, C., Champigneux, P., Renvoise, L., Audic, J.-M., Blanchet, E., Bergel, A., Bouchez, T., 2015. Successive bioanode regenerations to maintain efficient current production from biowaste. Bioelectrochemistry 106, 133–140. https://doi.org/10.1016/j.bioelechem.2015.05.007

Caporaso, J.G., Kuczynski, J., Stombaugh, J., Bittinger, K., Bushman, F.D., Costello, E.K., Fierer, N., Pena, A.G., Goodrich, J.K., Gordon, J.I., Huttley, G.A., Kelley, S.T., Knights, D., Koenig, J.E., Ley, R.E., Lozupone, C.A., McDonald, D., Muegge, B.D., Pirrung, M., Reeder, J., Sevinsky, J.R., Turnbaugh, P.J., Walters, W.A., Widmann, J., Yatsunenko, T., Zaneveld, J., Knight, R., 2010. QIIME allows analysis of high-throughput community sequencing data. Nat. Methods 7, 335–336. https://doi.org/10.1038/nmeth.f.303

Capson-Tojo, G., Rouez, M., Crest, M., Steyer, J.P., Delgenès, J.P., Escudié, R., 2016. Food waste valorization via anaerobic processes: a review. Rev. Environ. Sci. Biotechnol. 15, 499–547. https://doi.org/10.1007/s11157-016-9405-y

Conrado, R.J., Haynes, C.A., Haendler, B.E., Toone, E.J., 2013. Electrofuels: A new paradigm for renewable fuels, in: Advanced Biofuels and Bioproducts. Springer, pp. 1037–1064. https://doi.org/10.1007/978-1-4614-3348-4_38

Demler, M., Weuster-Botz, D., 2011. Reaction engineering analysis of hydrogenotrophic production of acetic acid by Acetobacterium woodii. Biotechnol. Bioeng. 108, 470–474. https://doi.org/10.1002/bit.22935

Deutzmann, J.S., Spormann, A.M., 2017. Enhanced microbial electrosynthesis by using defined co-cultures. ISME J. 11, 704–714. https://doi.org/10.1038/ismej.2016.149

Edgar, R.C., 2013. UPARSE: highly accurate OTU sequences from microbial amplicon reads. Nat. Methods 10, 996–998. https://doi.org/10.1038/nmeth.2604

Edgar, R.C., Haas, B.J., Clemente, J.C., Quince, C., Knight, R., 2011. UCHIME improves sensitivity and speed of chimera detection. Bioinformatics 27, 2194–2200. https://doi.org/10.1093/bioinformatics/btr381

El Mekawy, A., Hegab, H.M., Mohanakrishna, G., Elbaz, A.F., Bulut, M., Pant, D., 2016. Technological advances in CO2 conversion electro-biorefinery: A step toward commercialization. Bioresour. Technol. 215, 357–370. https://doi.org/10.1016/j.biortech.2016.03.023

Foulet, A., Bouchez, T., Desmond-Le Quéméner, E., Giard, L., Renvoisé, L., Aissani, L., 2018. Life cycle assessment of a bioelectrochemical system as a new technological platform for biosuccinic acid production from waste. Environ. Sci. Pollut. Res. 25, 36485–36502.

Gildemyn, S., Verbeeck, K., Slabbinck, R., Andersen, S.J., Prévoteau, A., Rabaey, K., 2015. Integrated Production, Extraction, and Concentration of Acetic Acid from CO2 through Microbial

Electrosynthesis. Environ. Sci. Technol. Lett. 2, 325–328. https://doi.org/10.1021/acs.estlett.5b00212

Hamelers, H.V.M., Ter Heijne, A., Sleutels, T.H.J.A., Jeremiasse, A.W., Strik, D.P.B.T.B., Buisman, C.J.N., 2010. New applications and performance of bioelectrochemical systems. Appl. Microbiol. Biotechnol. 85, 1673–1685. https://doi.org/10.1007/s00253-009-2357-1

Janicek, A., Fan, Y., 2014. Design of microbial fuel cells for practical application : A review and analysis of scale-up studies. Biofuels 5, 79–92. https://doi.org/10.4155/BFS.13.69

Jourdin, L., Grieger, T., Monetti, J., Flexer, V., Freguia, S., Lu, Y., Chen, J., Romano, M., Wallace, G.G., Keller, J., 2015. High Acetic Acid Production Rate Obtained by Microbial Electrosynthesis from Carbon Dioxide. Environ. Sci. Technol. 49, 13566–13574. https://doi.org/10.1021/acs.est.5b03821

Jourdin, L., Raes, S.M.T., Buisman, C.J.N., Strik, D.P.B.T.B., 2018. Critical Biofilm Growth throughout Unmodified Carbon Felts Allows Continuous Bioelectrochemical Chain Elongation from CO2 up to Caproate at High Current Density. Front. Energy Res. 6, 1–15. https://doi.org/10.3389/fenrg.2018.00007

Kim, M., Na, J., Lee, M., Ryu, H., Chang, Y., Triolo, J.M., Yun, Y., Kim, D., 2016. More value from food waste : Lactic acid and biogas recovery. Water Res. 96, 208–216. https://doi.org/10.1016/j.watres.2016.03.064

Koch, C., Harnisch, F., 2016. Is there a Specific Ecological Niche for Electroactive Microorganisms ? ChemElectroChem 3, 1282–1295. https://doi.org/10.1002/celc.201600079

Kracke, F., Kromer, J.O., 2014. Identifying target processes for microbial electrosynthesis by elementary mode analysis. BMC Bioinformatics 15, 410. https://doi.org/10.1186/s12859-014-0410-2

Lieder, M., Rashid, A., 2016. Towards circular economy implementation: A comprehensive review in context of manufacturing industry. J. Clean. Prod. 115, 36–51. https://doi.org/10.1016/j.jclepro.2015.12.042

Logan, B.E., Rabaey, K., 2012. Conversion of wastes into bioelectricity and chemicals by using microbial electrochemical technologies. Science 337, 686–690. https://doi.org/10.1126/science.1217412

Lovley, D.R., 2008. The microbe electric: conversion of organic matter to electricity. Curr. Opin. Biotechnol. 19, 564–571. https://doi.org/https://doi.org/10.1016/j.copbio.2008.10.005

Marshall, C.W., Ross, D.E., Fichot, E.B., Norman, R.S., May, H.D., 2012. Electrosynthesis of commodity chemicals by an autotrophic microbial community. Appl. Environ. Microbiol. 78, 8412–8420. https://doi.org/10.1128/AEM.02401-12

Nevin, K.P., Hensley, S.A., Franks, A.E., Summers, Z.M., Ou, J., Woodard, T.L., Snoeyenbos-West, O.L., Lovley, D.R., 2011. Electrosynthesis of organic compounds from carbon dioxide is catalyzed by a diversity of acetogenic microorganisms. Appl. Environ. Microbiol. 77, 2882–2886. https://doi.org/10.1128/AEM.02642-10

Nevin, K.P., Woodard, T.L., Franks, A.E., Summers, Z.M., Lovley, D.R., 2010. Microbial electrosynthesis: Feeding microbes electricity to convert carbon dioxide and water to multicarbon extracellular organic compounds. MBio 1, e00103-00110. https://doi.org/10.1128/mBio.00103-10

Pruitt, K.D., Tatusova, T., Maglott, D.R., 2007. NCBI reference sequences (RefSeq): A curated non-redundant sequence database of genomes, transcripts and proteins. Nucleic Acids Res. 35, D61–D65. https://doi.org/10.1093/nar/gkl842

Quast, C., Pruesse, E., Yilmaz, P., Gerken, J., Schweer, T., Yarza, P., Peplies, J., Glöckner, F.O., 2013. The SILVA ribosomal RNA gene database project: improved data processing and web-based tools. Nucleic Acids Res. 41, D590-6. https://doi.org/10.1093/nar/gks1219

Rabaey, K., Girguis, P., Nielsen, L.K., 2011. Metabolic and practical considerations on microbial electrosynthesis. Curr. Opin. Biotechnol. 22, 371–377. https://doi.org/10.1016/j.copbio.2011.01.010

Rabaey, K., Rozendal, R.A., 2010. Microbial electrosynthesis - revisiting the electrical route for microbial production. Nat. Rev. Microbiol. 8, 706–16. https://doi.org/10.1038/nrmicro2422

Sadhukhan, J., Lloyd, J.R., Scott, K., Premier, G.C., Yu, E.H., Curtis, T., Head, I.M., 2016. A critical review of integration analysis of microbial electrosynthesis (MES) systems with waste biorefineries for the production of biofuel and chemical from reuse of CO2. Renew. Sustain. Energy Rev. 56, 116–132. https://doi.org/10.1016/j.rser.2015.11.015

Schloss, P.D., Westcott, S.L., Ryabin, T., Hall, J.R., Hartmann, M., Hollister, E.B., Lesniewski, R.A., Oakley, B.B., Parks, D.H., Robinson, C.J., Sahl, J.W., Stres, B., Thallinger, G.G., Van Horn, D.J., Weber, C.F., 2009. Introducing mothur: open-source, platform-independent, community-supported software for describing and comparing microbial communities. Appl. Environ. Microbiol. 75, 7537–7541. https://doi.org/10.1128/AEM.01541-09

Straub, M., Demler, M., Weuster-botz, D., Dürre, P., 2014. Selective enhancement of autotrophic acetate production with genetically modified Acetobacterium woodii. J. Biotechnol. 178, 67–72. https://doi.org/10.1016/j.jbiotec.2014.03.005

Torres, C.I., Krajmalnik-Brown, R., Parameswaran, P., Marcus, A.K., Wanger, G., Gorby, Y.A., Rittmann, B.E., 2009. Selecting Anode-Respiring Bacteria Based on Anode Potential: Phylogenetic, Electrochemical, and Microscopic Characterization. Environ. Sci. Technol. 43, 9519–9524. https://doi.org/10.1021/es902165y

Venkata Mohan, S., Nikhil, G.N., Chiranjeevi, P., Nagendranatha Reddy, C., Rohit, M. V., Kumar, A.N., Sarkar, O., 2016. Waste biorefinery models towards sustainable circular bioeconomy: Critical review and future perspectives. Bioresour. Technol. 215, 2–12. https://doi.org/10.1016/j.biortech.2016.03.130

Villano, M., Monaco, G., Aulenta, F., Majone, M., 2011. Electrochemically assisted methane production in a biofilm reactor. J. Power Sources 196, 9467–9472. https://doi.org/10.1016/j.jpowsour.2011.07.016

Wang, H., Ren, Z.J., 2013. A comprehensive review of microbial electrochemical systems as a platform technology. Biotechnol. Adv. https://doi.org/10.1016/j.biotechadv.2013.10.001

Wang, Q., Garrity, G.M., Tiedje, J.M., Cole, J.R., 2007. Naïve Bayesian classifier for rapid assignment of rRNA sequences into the new bacterial taxonomy. Appl. Environ. Microbiol. 73, 5261–5267. https://doi.org/10.1128/AEM.00062-07

Xiang, Y., Liu, G., Zhang, R., Lu, Y., Luo, H., 2017. High-efficient acetate production from carbon dioxide using a bioanode microbial electrosynthesis system with bipolar membrane. Bioresour. Technol. 233, 227–235. https://doi.org/10.1016/j.biortech.2017.02.104

Zhilina, T.N., Zavarzina, D.G., Osipov, G.A., Kostrikina, N.A., Tourova, T.P., 2009. Natronincola ferrireducens sp. nov., and Natronincola peptidovorans sp. nov., new anaerobic alkaliphilic peptolytic iron-reducing bacteria isolated from soda lakes. Microbiology 78, 455–467.

https://doi.org/10.1134/S0026261709040092